Cape buffalo mitogenomics reveals a Holocene shift in the African human–megafauna dynamics

RASMUS HELLER,* ANNA BRÜNICHE-OLSEN† and HANS R. SIEGISMUND*

*Department of Biology, University of Copenhagen, Ole Maaløes Vej 5, 2200 Copenhagen N, Denmark, †School of Zoology, University of Tasmania, Private Bag 5, Hobart, Tas. 7001, Australia

Abstract

Africa is unique among the continents in having maintained an extraordinarily diverse and prolific megafauna spanning the Pleistocene–Holocene epochs. Little is known about the historical dynamics of this community and even less about the reasons for its unique persistence to modern times. We sequenced complete mitochondrial genomes from 43 Cape buffalo (*Syncerus caffer caffer*) to infer the demographic history of this large mammal. A combination of Bayesian skyline plots, simulations and Approximate Bayesian Computation (ABC) were used to distinguish population size dynamics from the confounding effect of population structure and identify the most probable demographic scenario. Our analyses revealed a late Pleistocene expansion phase concurrent with the human expansion between 80 000 and 10 000 years ago, refuting an adverse ecological effect of Palaeolithic humans on this quarry species, but also showed that the buffalo subsequently declined during the Holocene. The distinct two-phased dynamic inferred here suggests that a major ecological transition occurred in the Holocene. The timing of this transition coincides with the onset of drier conditions throughout tropical Africa following the Holocene Optimum ($\sim$9000–5000 years ago), but also with the explosive growth in human population size associated with the transition from the Palaeolithic to the Neolithic cultural stage. We evaluate each of these possible causal factors and their potential impact on the African megafauna, providing the first systematic assessment of megafauna dynamics on the only continent where large mammals remain abundant.

Keywords: Cape buffalo, climate change, demographic history, human activities, megafauna

Received 16 January 2012; revision received 9 April 2012; accepted 23 April 2012

Introduction

The persistence of a diverse and dominant megafauna to the present day in Africa is in sharp contrast to the late Pleistocene extinction of this community on other continents (Barnosky *et al.* 2004). Factors such as climate change, human hunting, disease epidemics and ecosystem collapse conceivably influenced megafauna dynamics to various degrees on different continents and much effort has been applied to establish their diverse impact on different continents (Barnosky *et al.* 2004; Nogués-Bravo *et al.* 2010; Lorenzen *et al.* 2011).

Not only might the successful evaluation of these drivers of historical megafauna population dynamics reveal important aspects of biogeographical history, it will also aid the understanding of the ecological background for the extinction processes within this prominent guild. The 'African anomaly' with respect to the persistence of a diverse megafauna to the present day has been attributed to the longer period of co-existence of humans and megafauna on this continent (Martin 1984), but there is little direct evidence of benign human-megafauna relations in Africa. Studies of the Pleistocene extinctions previously relied on the fossil record, but an increasing number of studies use genetic data to infer species population size dynamics, which can then be compared to known periods of climate change and human

Correspondence: Rasmus Heller, Fax: (+45) 35321300;
E-mail: rheller@bio.ku.dk

demographics or presence/absence in a given region to infer causal relations (e.g. Shapiro *et al.* 2004; Goossens *et al.* 2006; de Bruyn *et al.* 2009; Campos *et al.* 2010). This approach holds promise in assessing the susceptibility of the megafauna to the two most prominent threats to its persistence, climate change and human activities.

As opposed to the other continents, humans (the term 'humans' is used in the sense of anatomically modern humans throughout) have co-existed with the African megafauna for hundreds of thousands of years. African humans certainly hunted the megafauna in the late Pleistocene (Faith 2008; Dusseldorp 2010), but the ecological effect of this is unknown. The fact that humans co-existed with the buffalo for a long time in Africa allows us to test the hypothesis of benign ecological relations by comparing the dynamics of both species throughout the late Pleistocene and the Holocene. Comparisons over such an extensive period are not possible on other continents because of the late arrival of modern humans elsewhere.

The purpose of this study was to evaluate the effect of humans and climate change on the Cape buffalo, a large and widespread ungulate distributed at relatively high densities throughout most of eastern and southern Africa (Sinclair 1977). The buffalo is a convenient model for the effects of climate change and human activities, as it is a Palaeolithic quarry species (Faith 2008; Dusseldorp 2010) and has been shown to be susceptible to drought (Ogutu *et al.* 2008), which is the most ecologically important climate variable in tropical Africa. Previous studies using autosomal microsatellites and fragments of the mitochondrial D-loop fragments have found genetic signals of both a population expansion (Van Hooft *et al.* 2002) and a population decline (Heller *et al.* 2008), which appears contradictory. However, the expansion was inferred to have occurred in the Pleistocene and the decline in the Holocene, so it is possible that the buffalo has gone through a two-phased dynamic similar to the steppe bison (Shapiro *et al.* 2004; Drummond *et al.* 2005). Tentative evidence from two other African savannah-adapted mammals—the savannah elephant and the baboon—has shown that they also suffered severe population decline in the Holocene or late Pleistocene (Storz *et al.* 2002; Okello *et al.* 2008), raising the possibility that this was a time of a community-wide collapse.

We present here the first complete mitochondrial genome (mitogenome) sequences from the Cape buffalo. Recent studies have shown that mitogenome sequences may reveal the aspects of history not discernible by analysing only smaller regions such the D-loop (Morin *et al.* 2010; Wang *et al.* 2010). Although generally assumed to be a single, non-recombining locus, complete mitogenomes provide more variable sites, hence more information to be utilized in the analyses of demographic history. Specifically, the faster accumulation of substitutions in the complete mitogenome compared to mitogenome fragments provides improved time resolution for historical inferences using molecular clock approaches. It should be noted, though, that the inclusion of several unlinked genetic markers would improve the demographic inferences even further (reviewed in Ho & Shapiro 2011).

Most methods aiming at inferring population size dynamics by applications of coalescent theory make simplifying assumptions about the biological system, notably about the underlying population structure. Although the potentially confounding effect of population structure on inferences of population size changes has been made clear in a number of mainly theoretical studies (e.g. Wakeley 1999, 2000; Pannell 2003; Ray *et al.* 2003; Städler *et al.* 2009; Chikhi *et al.* 2010; Ho & Shapiro 2011), it is underappreciated in practical studies using real data. Essentially, when population structure does exist, the migration of genetic lineages among subpopulations can alter the expected waiting times between coalescence events upon which such methods rely to infer dynamics in population size. It is difficult to evaluate the confounding effect of population structure a priori, but one way of assessing it is by simulating data under different structural scenarios and comparing the inferences under these scenarios with the signal observed from the observed data. This approach was adopted in various ways in the present study, allowing us to evaluate the robustness of the inferences of population size dynamics presented here.

Materials and methods

Sampling and laboratory procedure

Samples were collected from three localities within the Cape buffalo distribution: Omo Valley in Ethiopia (n = 7); Masai Mara in Kenya (n = 20) and Chobe/Hwange national parks in Botswana/Zimbabwe (n = 16). This sampling scheme was chosen in part to avoid strictly 'local' sampling as pointed out by e.g. Städler *et al.* (2009) and Chikhi *et al.* (2010). Details about sample collection methods can be found in Simonsen *et al.* (1998). Two primer sets were designed to amplify the complete mitochondrial genome for the buffalo by aligning 20 published mitogenomes from a range of bovid species using the built-in alignment function in GENEIOUS (Drummond *et al.* 2010) with the 70% similarity cost matrix. Conserved sequence regions that were amenable for primer design were identified by eye and by using the Primer3 software (Rozen & Skaletsky 2000). The

primer sequences are as follows: (1_F: GAGCCTTCA AAGCCCTAAGC; 1-R: CGGATTTTCCNGTTGCRGC; 2_F: CAGARCGYCTAAACGCCG; 2_R: CGGGAGAAG-TAGATTGAAGCC). The two fragments were 7448 nt and 10 912 nt long, respectively, and overlapped by ~200 nt and 1800 nt at either end. Long-range PCRs were carried out using the Platinum® *Taq* High Fidelity PCR kit (Invitrogen). PCR products were run on agarose gel to verify the length of the product. Amplicons with a clear band at the expected length were PCR purified using the MSB Spin PCRapace kit (STRATEC) and sent for library preparation and sequencing at BGI, Shenzhen, China. Here they were Illumina sequenced using paired-end technology. Raw sequence data were assembled using the de novo assembly algorithm of SOAPDENOVO (Li *et al.* 2010) with parameters '–k 27 –d 1' and, for some samples that could not be de novo assembled, by reference-guided assembly using one of the de novo assembled sequences as a reference in GENEIOUS with the default parameters under medium sensitivity. For the reference-assembled mitogenomes, we used several different reference mitogenomes to evaluate the effect of this on the final sequence. All assembled genomes were blasted and aligned to existing buffalo mitochondrial DNA sequences to check them for inter-species contamination. We also aligned the assembled mitogenomes to reference cattle (NC_006853) and water buffalo (NC_006295) mitogenomes to check them for dubious indels or other potential artefacts. The assembled mitogenomes were annotated according to the above published reference mitogenomes from cattle and water buffalo.

Demographic analyses

The assembled mitogenomes were partitioned into three regions: (i) protein-coding sequence, consisting of 12 protein-coding genes ND1, ND2, COX1, COX2, ATP8, ATP6, COX3, ND3 ND4L, ND4, ND5 and CYTB (excluding the ND6 gene situated on the heavy strand); (ii) two rRNA genes s-rRNA and l-rRNA; and (iii) the D-loop region. We also used a combined data alignment with these three regions concatenated into a single unpartitioned sequence. A more elaborate partitioning scheme where each gene was allowed a separate model of evolution was also explored. JMODELTEST (Posada 2008) was used to evaluate the most appropriate model of evolution for each alignment and partition according to the Akaike Information Criterion. As recombination can bias inferred genealogies (Schierup & Hein 2000), we tested for the presence of recombination in the mitogenomes using the GARD and SBP methods (Pond *et al.* 2006) implemented at the DataMonkey webserver.

To calibrate the substitution rate of the partitions, we aligned the buffalo partitions to published cattle mitogenome NC_006853 from which the divergence time of the bubalina subfamily has recently been estimated based on the fossil record (7.7 mya (MacEachern *et al.* 2009)). These alignments were analysed using BEAST (Drummond *et al.* 2005, 2006) under the assumption of a relaxed (log-normal distributed) molecular clock. From this, we obtained the age of the Cape buffalo genealogy (mean and 95% HPD) and used this node as a prior to calibrate subsequent BEAST analysis involving the buffalo demographic history. We used the extended Bayesian skyline plot (EBSP (Heled & Drummond 2008)) demographic tree prior in BEAST and ensured convergence by running the program long enough to get effective sample sizes of at least 500 for all parameters. The EBSP was developed to accommodate multilocus data, but it was chosen here because we wanted to estimate the unique EBSP parameter PopulationSizeChanges (PSC; Fig. S1, Supporting information), which quantifies the number of demographic changes most in agreement with the data. The two alternative Bayesian skyline methods currently available in BEAST (the Bayesian skyline plot, BSP (Drummond *et al.* 2005) and the Gaussian Markov random field skyride, GMRF (Minin *et al.* 2008)) were also explored to evaluate the effect of the skyline demographic prior, and the inferred history proved very similar across methods (Fig. S2, Supporting information). Different concatenation schemes were explored by running (i) a concatenated data set including all three partitions, but allowing substitution models to vary between the partitions; (ii) each of the three partitions by itself (not concatenated); (iii) a concatenated data set allowing substitution models to vary between each gene; and (iv) a pooled data set applying the same substitution model across the whole length of sequence. Under all concatenation schemes, the outgroup alignment was run first and the root posterior of the Cape buffalo genealogy from the outgroup analysis was used as calibration prior for the EBSP analyses. A strict molecular clock was assumed throughout the following, as exploratory runs did not support a relaxed clock.

To evaluate the effect of human activities and climate change on the inferred buffalo history, we collected proxy data for these two factors. An estimate of sub-Saharan human population sizes through time was kindly provided by Quentin D. Atkinson (Atkinson *et al.* 2008). As precipitation (rather than temperature) is the most ecologically important climatic variable in tropical Africa (Ogutu *et al.* 2008), we obtained an estimate of the amount of yearly precipitation over time from sediment records from the Lake Tanganyika basin in Central Africa (Tierney *et al.* 2010). Finally, we collected and analysed a data set of indigenous Ethiopian cattle (Dadi *et al.* 2009) to compare the population

dynamics of livestock with that of the buffalo (Supporting information).

We applied a correction factor for the time points in the skyline plot functions to account for substitution rate decay over evolutionary time scales (Ho *et al.* 2005). For this we used the time-dependent correction factor from Gignoux *et al.* (2011) to estimate the ratio of short-term to long-term rate at each time point inferred under the skyline models. This ratio was used to re-calculate the coalescent intervals in the skyline functions by dividing each interval with the appropriate ratio, arriving at a new calibrated set of time points for the skyline plots. Although strictly only applicable for human mitogenomes, we used this calibration as a general approximation for correcting the decay of rates for the buffalo data as well as the human data in Figs 1, 3, S2 and S3 (Supporting information).

Simulated scenarios and comparison with the observed data

Because different types of demographic processes can give rise to apparent population size changes in a skyline plot (Supporting information), and because we wanted to test the robustness of skyline plot methods, we used data simulations to explore the skyline signal of a number of competing demographic scenarios. Two series of scenarios were considered: one (four scenarios; Sce1a–d) entailing different histories of population size change and one (three scenarios; Sce2a–c) consisting of different types of structure with or without any changes in the total population size (Fig. 2, Supporting information). A number of additional scenarios were explored, but are not included in the study because they did not provide a good fit to the observed data
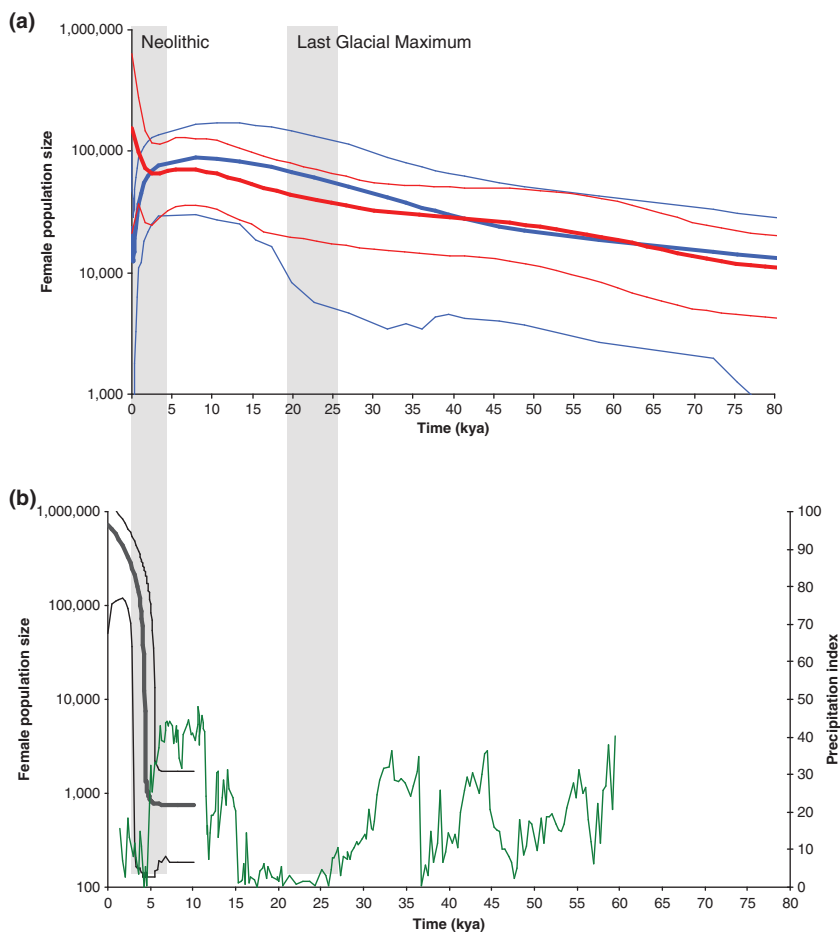

Fig. 1 Comparing buffalo, human and cattle population size and precipitation through time. (a) Extended Bayesian skyline plot (EBSP) from buffalo data (blue) with Bayesian skyline plot (BSP) of sub-Saharan humans (red; modified from Atkinson *et al.* (2008)). (b) EBSP of African cattle (Dadi *et al.* (2009); black) and data on estimated precipitation patterns in Tanzania (Tierney *et al.* (2010); green). The skyline plots show mean effective female population sizes (bold lines) and 95% HPD intervals (thin lines). The time unit is kya (thousands of years before present). The buffalo EBSP is based on the unpartitioned data (see text for further details). The population size axis is on logarithmic scale; raw values from BEAST are in units of N_E*g and have been divided by generation time. Insert are two key historical events: the Last Glacial Maximum and the Neolithic period.
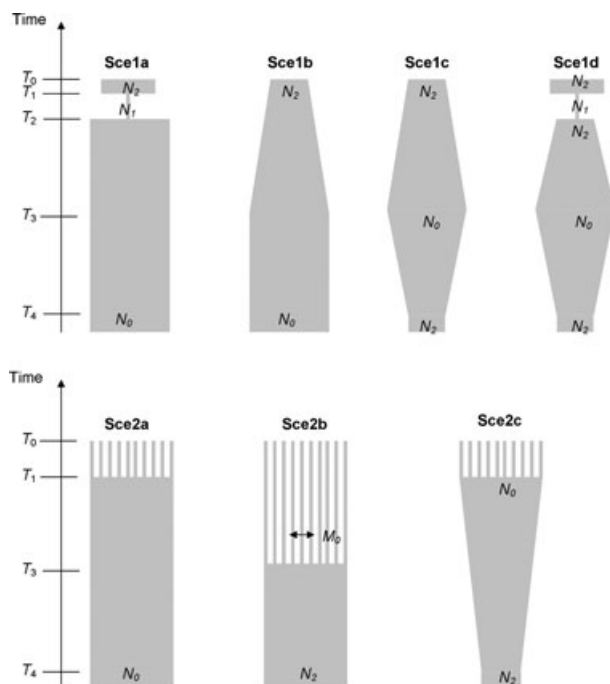
Fig. 2 Scenario overview. Scenario abbreviations can be found in Table 2, and parameter values are in Table 3. Details about each scenario are provided in the Supporting information. The time axis is shown for clarity and is not to scale.

and were not concordant with the known history of the buffalo.

Scenario 1d was included as a 'positive control' to assess the ability of the EBSP to pick up a complex signal such as the one inferred from the real data. For each scenario, 100 data sets corresponding to the unpartitioned real data (43 samples, 16 400 bp evolving according to the HKY + G substitution model inferred with JMODELTEST using parameter values as inferred in BEAST) were simulated using Bayesian Serial SimCoal (BSSC (Chan *et al.* 2006)). This software was used because of its flexibility in model specification, the possibility of putting priors on model parameters and the ease of piping the output into ABCtoolbox (Wegmann *et al.* 2010; see below). The simulated data sets were analysed in BEAST using EBSPs, and plots depicting EBSP of each replication of the different scenarios were made using R. To further investigate the effect of sampling in the presence of population structure, we randomly subsampled 25 individuals from the full set of 43 one hundred times and did EBSP analysis on them. The resulting plots are shown in Fig. S4 (Supporting information).

Approximate Bayesian computation (ABC) analyses were performed to test the fit of the alternative scenarios mentioned above to the data. This entails simulating data under the different scenarios, extracting a suite of summary statistics from the simulated data and com-

paring the value of these statistics with the values of the same statistics calculated from the observed data (Beaumont 2010). The scenario yielding summary statistics most similar to those from the observed data is regarded as the most compatible with the data. We used the ABCestimator component of the ABCtoolbox package to assess the different scenarios and performed model selection by comparing the marginal density of each scenario. The summary statistics included in the analyses (following a selection procedure excluding tightly correlated and uninformative statistics) were the number of haplotypes, nucleotide diversity, Tajima's D and the time of the most recent common ancestor (TMRCA). The values of these statistics in the observed data were calculated using DNASP (Rozas *et al.* 2003) for the first three and the mean estimate of the tree root height in BEAST for the latter. For each scenario, 10^5 simulation steps were carried out, and we retained the best 5000 for the calculation of marginal density and P-value. Model selection was performed by computing Bayes factors based on the marginal densities of each scenario. The relative probability was calculated by combining the 5000 retained simulation steps from each scenario (total 35 000 retained simulation steps), sorting them by distance to the observed data set and calculating the proportion of each scenario among the top 7000 steps, following Pritchard *et al.* (1999).

The posterior distributions of the parameters N_0, N_1/N_2 (rinderpest bottleneck severity), N_2, T_3 and T_4 in scenario 1d (Fig. 2) were estimated to validate the inferred population size changes observed in the skyline plots. Parameters T_1 and T_2 are determined by known historical events and were fixed to known values (Table 3).

Results

Mitogenomic diversity

The 43 Cape buffalo mitogenomes were 16 357–16 361 bp in length (with the exception of a single Ethiopian individual, 9083, having a 74 bp deletion in the D-loop shortening the mitogenome to 16 285 bp) and have been submitted under GenBank accession numbers JQ235505–JQ235547. The mitogenomes consisted of 30 different haplotypes and had a nucleotide diversity of 0.0045 (Table 1). Tajima's D was −1.25, which was not significantly different from zero. No evidence of recombination was found in the mitogenomes. The inferred rate of change over the complete mitogenome using the divergence from cattle as calibration points was 3.1×10^{-2} per site per Myr (95% HPD: 2.4–4.0×10^{-2}), which is very close to the mean across mammals (3.3×10^{-2} per site per Myr (Nabholz *et al.*

Table 1 Genetic diversity of the mitogenomes

Population	Samples	Seg. sites	Haplotypes	π	Tajima's D
Omo Valley	7	162	7	0.00348	−0.87
Masai Mara	20	260	14	0.00353	−0.91
Chobe/Hwange	16	276	10	0.00476	−0.30
Combined	43	456	30	0.00435	−1.24

Seg. sites: number of segregating sites; π: nucleotide diversity.

2008), but considerably slower than that of humans (6.8×10^{-2} per site per Myr externally calibrated (Endicott & Ho 2008)). This yielded a time since most recent common ancestor (TMRCA) of 110 kya (95% HPD: 81–144 kya) for the Cape buffalo.

Inferred population size dynamics

The EBSP revealed a history of variable population size in the Cape buffalo with a notable expansion and decline phase, respectively (Fig. 1a). Skyline plots based on different partitioning schemes were very similar (Fig. S3, Supporting information), justifying the compatibility of the results derived from BEAST and the ABC analyses (where unpartitioned data were used). The first part of the history shows a general population expansion starting at the lower 95% highest probability density (HPD) interval of the root age at ~80 kya, progressing until a peak population size ~8 kya. From this time we observe a moderate decline accelerating to a rapid and precipitous decline within the last 5000 years. The 95% HPD interval around the mean inferred population size was incompatible with a constant population size through time, and the posterior median for the parameter PopulationSizeChanges (PSC; representing the number of population size changes in the EBSP) was 3 with 95% HPD 2–4, strongly rejecting a constant population size even though the prior on this parameter gave equal support to a constant vs. all non-constant population histories (all possible non-zero values of PSC). The three skyline plot methods (EBSP, GMRF and BSP) showed very similar trajectories, although the peak in population size was slightly older in the EBSP than under the other models (Fig. S2, Supporting information).

Comparison with simulated data

The scenarios on which simulations were based are shown in Fig. 2. The EBSPs based on the simulated data (Fig. 3) show that scenario Sce1d (the 'positive control') produced plots closely resembling the EBSP from the observed data, with scenarios Sce1c and Sce2c also capturing some aspects of the observed signal. None of the remaining scenarios yielded EBSPs visibly similar to the observed. The EBSP method was quite accurate in picking up the demographic signal encoded in the simulated data. Given that the EBSP method essentially integrates over all possible demographic functions, our results confirm that the method is evidently able to pick up a demographic signal in the type of data we have simulated (emulating mitogenomes). The structure scenarios yielded quite variable EBSP plots including signals of population expansion, decline and stability, and this underlines the potentially confounding effect of structure on demographic inference. Among the scenarios involving population structure, Sce2b overestimated the number of population size changes (Fig. S3, Supporting information). This demonstrates that structure can mimic population size changes and shows that structure must be of a certain age to leave a false signal of population size change, in agreement with Fig. 2a in Peter *et al.* (2010).

Approximate Bayesian Computation was carried out as a further test of the demographic scenarios. The same scenarios as above were evaluated, and the fit between simulated summary statistics under each scenario and those from the observed data are compared in Table 2. Scenario 1d was the best fit to the observed data with a *P*-value of 0.98 and a Bayes factor of 4.4 favouring this over the second best model (Sce1c). The main virtue of Sce1d compared to Sce1c appeared to be its ability to explain the relatively low number of haplotypes (30 haplotypes among 43 samples). A high number of identical haplotypes compared to other mismatch classes are indicative of a very recent bottleneck (when structure can be excluded). The posterior estimates of the times of demographic changes are shown in Table 3 and are in good agreement with the skyline plot results, confirming that the data are informative regarding these model parameters both under full likelihood methods and using summary statistics.

Discussion

Methodological evaluation

The list of studies using different varieties of skyline plots to infer historical population size dynamics is
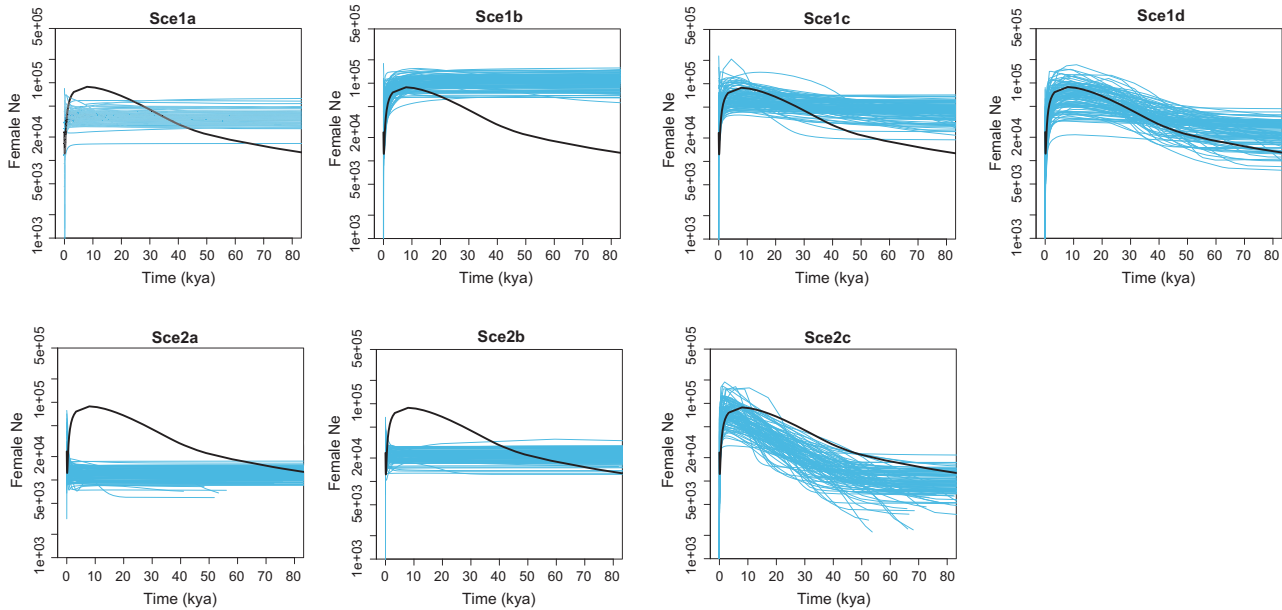
Fig. 3 Simulated data EBSPs. Scenario abbreviations as per Table 2 and Fig. 2. The inferred EBSP from the real data (Fig. 1a) is included in all panels (black line), EBSP mean values from 100 data sets based on each scenario is shown in blue. Sce1a–d series (upper panel) are scenarios without structure, Sce2a–c series (lower panel) are scenarios with biologically realistic population structure.

growing fast, but many of these studies do not explicitly consider alternative demographic processes that may have given rise to the skyline signal. Particularly, it is well known that population structure can have a strong effect on the underlying genealogy, leaving a signal resembling that of a population decline. To our knowledge, our study is the first to perform BSP analyses on simulated data from a range of competing and plausible demographic scenarios. Other authors dealing with empirical data have addressed

Table 2 Scenario overview and ABC results

Scenario	Marginal density	*P*-value	Relative probability
Sce1a	0.053	0.516	0.16
Sce1b	0.000	0.000	0.00
Sce1c	0.097	0.736	0.15
Sce1d	0.432	0.983	0.55
Sce2a	0.041	0.554	0.01
Sce2b	0.000	0.030	0.02
Sce2c	0.045	0.860	0.11

the issue of structure in other ways (e.g. Städler *et al.* 2009; Campos *et al.* 2010; Chikhi *et al.* 2010; Peter *et al.* 2010; Hoffman *et al.* 2011; Lorenzen *et al.* 2011). We affirm that a confounding effect of population structure on inferred skyline plots should routinely be

examined, especially considering the popularity of these methods. We used simulations to assess the probability of alternative demographic and structural scenarios creating the genetic signal observed in skyline plots and in the summary statistics. None of the alternative scenarios considered here yielded signals resembling those in the observed data (Fig. 3). We also explored other variants of the main scenarios listed here, but none were a better fit to the data than those presented here. The use of simulations allowed us to exclude some of the most obvious alternative explanations for the observed pattern of genetic diversity, making us more confident that the skyline plots in Figs 1, S2 and S3 (Supporting information) are a good approximation of the actual historical dynamics of the Cape buffalo, not just artefacts of structure and sampling. Although not the main focus of this study, our EBSP analyses using controlled simulations revealed several interesting aspects concerning the precision and robustness of this method in inferring demographic history. Given the popularity of skyline plot methods, further simulation studies on this topic are warranted. We acknowledge that the shifting buffalo range contractions and expansions caused by human activities and climate change may have caused more complex changes over time in genetic structure and diversity than we were able to simulate (Excoffier *et al.* 2009; Arenas *et al.* 2011), but it was outside the scope of this study to incorporate such a level of complexity.

Table 3 Scenario parameters: posteriors and priors from ABC analysis of Sce1d

Parameter	Prior	Mode/value[*]	Posterior[†] (95% HPD)
N_0[‡]	10 000–500 000	110 156	55 190–167 080
N_1/N_2	0.02–0.10	0.087	0.056–0.100
N_2	1000–50 000	11 016	5520–16 709
T_1	NA	100	NA
T_2	NA	130	NA
T_3	3500–21 000	5898	3668–12 401
T_4	50 000–100 000	79 114	61 950–87 145
M_0	NA	0.0003	NA

[*]The mode of the posterior distribution or the fixed value of the parameter if not estimated.
[†]The posterior estimates are based on the most probable demographic scenario, Sce1d. All times are in years; all effective population sizes are in natural units.
[‡]N_0 was fixed at 10-fold larger than N_2 and is hence not an independent variable.
NA, not applicable; parameter was fixed to a value and not estimated; HPD, highest probability density.

It should be stressed that the time resolution of the inferred demographic history is not sufficient to pinpoint the exact dates of demographic change points. Uncertainty about the calibration of divergence time between the bovina and bubalina subfamilies and the potential bias in using ancient calibration points to inform on recent intraspecific rates of evolution both influence the rate of the molecular clock assumed in the historical inference (Ho *et al.* 2005; Endicott & Ho 2008). The latter source of bias was controlled by applying a correction factor for the decay of substitution rates over evolutionary time (Gignoux *et al.* 2011). Also, we note that our estimate for the TMRCA of the Cape buffalo (81–144 kya) agrees with that inferred assuming a substitution rate calibrated from ancient DNA from a closely related species (the bison; Shapiro *et al.* 2004) and using a much larger Cape buffalo D-loop sample (85–192 kya, data available from the authors). Overall, however, we can hardly pinpoint demographic change points with less than some thousand years of uncertainty. This lack of temporal resolution precludes us from tying the inferred history to specific historical events with certainty (see below), a problem confronting all studies attempting to correlate inferred events in species histories with external events. We also acknowledge that having more unlinked loci instead of the one non-recombining sequence of the mitogenome would significantly improve our demographic inference. The mitogenome represents just one realisation of the coalescent process and is restricted to the matriline. However, with regard to the Holocene decline, our

mitogenome results agree closely with previous results from autosomal microsatellites (Heller *et al.* 2008).

Cape buffalo demographic history I: reconciling previous findings

The sequencing of complete mitogenomes allowed us to gain a more detailed insight into the demographic history of the Cape buffalo and shows that it is possible, even using only modern DNA sequences, to infer complex dynamics of demographic history. Collectively, our BEAST analyses and the ABC procedure suggest that a model including a Pleistocene expansion (starting around 80 kya) followed by Holocene decline (starting around 5 kya) and a bottleneck caused by the rinderpest epidemic in the late nineteenth century is the most plausible among a range of biologically relevant scenarios for the Cape buffalo. This dynamic reconciles previous findings (Van Hooft *et al.* 2002; Heller *et al.* 2008), although we acknowledge that it is not necessarily surprising to get discrepant demographic signals from markers with different inheritance mode (as well as between unlinked markers sharing inheritance mode). We also found a genetic signal of the historically well-documented rinderpest epidemic (references in Estes (1991)), which has so far not been detectable using other methods of demographic inference. Excoffier & Schneider (1999) note how a recent bottleneck can erase or mitigate the signal of an earlier expansion. This might explain why tests based on Tajima's *D* and Fu's *F* fail to find significant support for a Pleistocene expansion in buffalo despite showing a tendency towards an expansion signal.

Cape buffalo demographic history II: explosive human growth or climate change?

Our results reveal two aspects of buffalo dynamics of particular interest when compared with that of African humans: a concordant increase in effective population sizes of these two species from around 80–10 kya and a radical divergence in the dynamics of the species from around 5 kya onwards (Fig. 1). This divergence is marked by the onset of explosive growth in the human population size, a well-known feature of human demographic history (Atkinson *et al.* 2008, 2009; Barnosky 2008; Scheinfeldt *et al.* 2010; Gignoux *et al.* 2011; Soares *et al.* 2012), and a correspondingly rapid decline in the buffalo population size. The first phase of this interspecies dynamic reveals that Palaeolithic humans did not have an adverse impact on the buffalo, although they certainly hunted the species on occasion (Faith 2008; Dusseldorp 2010). On the contrary, humans and buffalo both expanded by a factor of about five between 80 and

10 kya. This suggests favourable climate change or a common recovery from a contemporaneous bottleneck. The former is supported by evidence that the climate in tropical Africa recovered from a series of megadroughts during 135–75 kya to a subsequently more stable and moist climate (Cohen *et al.* 2007; Scholz *et al.* 2007). The latter is supported by the hypothesis of a volcanic winter causing significant ecosystem breakdown 74 kya, following the violent eruption of Toba in present day Indonesia (Rampino & Self 1992; Ambrose 1998). Toba was the largest volcano eruption registered in the Pleistocene, and several authors have hypothesized that it was responsible for the bottleneck in humans around this time (Ambrose 1998). It is plausible that many species were reduced to low population sizes during this climatic disturbance only to recover and expand once conditions became more benign. As the two hypotheses are not mutually exclusive, we restrict our conclusions regarding the Palaeolithic period (80–10 kya) to state that neither humans nor climate conditions posed a serious ecological threat to the buffalo. Indeed, there is evidence to suggest that the period from ∼70 kya to ∼20 kya, the height of the most recent glacial period, was characterized by increasingly open vegetation types around tropical Africa at the expense of closed forest (Hamilton & Taylor 1991).

The onset of the second and markedly different phase in the buffalo history is concordant with the last great extinction pulse for megafauna on other continents (Barnosky 2008). Following the rationale that there is a limited carrying capacity for all of the megafauna (humans included), Barnosky takes a global view on this and suggests that this period of mass extinction signifies a threshold event pushing the ecosystem state into a new stable 'basin of attraction', where humans and their domesticates started dominating the megafaunal biomass at the expense of all other species (Fig. 1). In the case of the African continent, there are two likely explanations for such an ecological shift: the Neolithic revolution and Holocene aridification.

The Neolithic revolution. The Neolithic revolution occurred in northern Africa about 10 kya and probably (although this is subject to considerable uncertainty) spread to east Africa and the Sahel region no later than ∼4.5 kya (Scheinfeldt *et al.* 2010), possibly simultaneously with the Bantu expansion (Soares *et al.* 2012). The cultural transition of African humans from the Palaeolithic to the Neolithic, characterized by the adoption of pastoralism and agriculture (Scheinfeldt *et al.* 2010), may have transformed a previously benign ecological co-existence of humans and buffalo to a negative impact. This could be due to an increase in human activities and land use due to the acquisition of pasto-

ralist practise, a critical threshold of human population size (Fig. 1) being reached that disrupted the ecological balance, or a combination of these. Alternatively, or additionally, cattle pastoralism may have introduced novel diseases to which the Cape buffalo had little immunity (the hyperdisease hypothesis; reviewed in Koch & Barnosky (2006)). A recent and well-documented example of the latter is the rinderpest pandemic, which swept Africa in the late nineteenth century following the introduction of cattle from the Indian subcontinent, decimating the buffalo population by >90% (Estes 1991). Analyses of African cattle demographic history confirm that cattle populations increased rapidly following the Neolithic revolution and follows a remarkably concurrent, but opposite trend from the buffalo in the Holocene (Fig. 1B; Finlay *et al.* 2007).

Holocene aridification. The onset of a general aridification of Africa in the mid-Holocene may have caused increased mortality in the Cape buffalo. Although not as extreme as some periods of the Pleistocene (see precipitation history plot in Fig. 1), the Holocene has witnessed periods of considerable and quite rapid climate change (Mayewski *et al.* 2004; Thompson *et al.* 2006; de Bruyn *et al.* 2011). This applies particularly for Africa, which went through a very pronounced aridification following the relatively warm and wet Holocene Climatic Optimum ∼9–5 kya (deMenocal *et al.* 2000; Thompson *et al.* 2002; Tierney *et al.* 2010). At this time, the previously savannah-covered Sahara region deteriorated into the desert we see today, and a number of large lakes and waterways in the region dried up completely. Underlying this general aridification are at least two specific events, the 5.9 kya and 4.2 kya events (Brooks 2006), which many sources identify as extremely sudden and pronounced drought periods. The latter has been termed as the 'First Dark Age' of human civilization and caused major upheaval in early cultures in the Middle East, Egypt, China and the Americas (deMenocal 2001). It was associated with extreme drought in the entire Nile catchment area and a temporary cessation of the flow of the Nile because of low lake levels along the course of the White Nile (Stanley *et al.* 2003; Williams & Talbot 2009). The Cape buffalo is known as one of the most water dependent of the savannah ungulates (Ogutu *et al.* 2008), and climate change in the Holocene was definitely severe enough to have had profound ecological consequences (Mayewski *et al.* 2004). The demographic history presented here is in agreement with the hypothesis that the mid-Holocene aridification of Africa posed a serious challenge for many drought-intolerant species of savannah ungulates (Heller *et al.* 2008).

The present evidence does not enable us to directly assess the contribution of these two possible causal factors for the buffalo population decline. One obvious argument against Holocene climate change as the sole causal agent is the fact that the above episodic droughts, although historically recorded as dramatic, were almost certainly not as pronounced as those recorded in the Pleistocene (Fig. 1), for example, associated with the Last Glacial Maximum ~26.5–19 kya (Wolff *et al.* 2011), a period where the buffalo population was still expanding. Therefore, there seems to be compelling evidence for at least some human contribution—quite possibly in concert with Holocene climatic pertubations—to the collapse of the Cape buffalo population in the Holocene. Under this scenario, the pressure from rapidly expanding human activities combined with the Holocene aridification, which although not the most severe recorded was certainly enough to affect the Cape buffalo, led to a negative population growth rate for the buffalo. It is even possible that the Holocene aridification drove humans and megafauna into closer contact around remaining water sources, hence forcing them to share the same fragmented habitat and throwing them into increased ecological competition in which the megafauna was bound to lose as human populations entered an explosive growth phase.

Shedding light on the African anomaly

Africa is key to understanding the global patterns, if such exist, of megafauna dynamics underlying the global mass extinction at the Pleistocene–Holocene transition. No other continent can provide as complete and extensive a record of human–megafauna co-existence as Africa. Yet, African megafaunal history remains severely understudied in comparison with its temperate and Arctic counterparts. This study provides evidence—beyond the mere persistence of megafauna diversity in Africa—of ecologically benign co-existence of Palaeolithic humans and a prominent member of the African megafauna, underlining that the ecological impact of humans in prehistory may have been complex and was certainly not uniformly harmful. The hypothesis of an ecological state transition from benign co-existence to human–megafauna competition following the Neolithic revolution is tantalizing and warrants further investigation.

Although still tentative, this study raises the possibility that the African megafauna underwent a population collapse equivalent to and roughly contemporaneous with that on other continents (Barnosky 2008). Hence, the history of the African megafauna may not be as exceptional as previously assumed, disregarding that the Holocene decline did not result in as many species

extinctions as on other continents. Explanations for this aspect of the African anomaly must be speculative, but one possibility is that Africa offered more suitable refugia from human activities than other continents. Such refugia could stem from the vastness and physical heterogeneity of the African landmass within the species-rich tropics, or the existence of pathogens that precluded humans or domesticates from thriving in certain areas. The latter is still true as exemplified by the persistence of locally endemic livestock diseases such as animal trypanosomiasis and several others, making large tracts of otherwise attractive pasturelands in Africa unavailable to human settlement, a phenomenon without parallel on other continents.

It should be noted that genetic studies on the megafauna of other continents suggest that species may have responded idiosyncratically to climate change and human activities. For some species (elephant seal, musk ox, woolly rhino), climate change appears to be sufficient to explain their inferred dynamics (de Bruyn *et al.* 2009; Campos *et al.* 2010; Lorenzen *et al.* 2011), but for others (steppe bison, wild horse), a human contribution cannot be excluded (Drummond *et al.* 2005; Lorenzen *et al.* 2011). It remains an open question to what extent community-wide or continental patterns of megafauna response to climate change and human activities exist. Ultimately, the only way to test this is to study more species in a comparative context. Although other members of the African megafauna have shown demographic histories compatible with a major ecological transition in the Holocene (Storz *et al.* 2002; Okello *et al.* 2008), more research is needed to establish whether the demographic history of the buffalo is representative of the community. Particularly, we do not yet know to what extent structure may have biased the few studies published on other African species. Future work will help to evaluate whether humans generally co-existed peacefully with the megafauna in the Palaeolithic Africa, and whether Holocene climate change or a human cultural evolution has been more influential in shaping the history of this community. As more genetic data become available, particularly multi-locus genomic data, it will hopefully be possible to carry out more accurate, community-wide inferences of demographic history.

References

Ambrose SH (1998) Late Pleistocene human population bottlenecks, volcanic winter and differentiation of modern humans. *Journal of Human Evolution*, **34**, 623–651.

Arenas M, Ray N, Currat M, Excoffier L (2011) Consequences of range contractions and range shifts on molecular diversity. *Molecular Biology and Evolution*, **29**, 207–218.

Atkinson QD, Gray RD, Drummond AJ (2008) mtDNA variation predicts population size in humans and reveals a major southern Asian chapter in human prehistory. *Molecular Biology and Evolution*, **25**, 468–474.

Atkinson QD, Gray RD, Drummond AJ (2009) Bayesian coalescent inference of major human mitochondrial DNA haplogroup expansions in Africa. *Proceedings of the Royal Society of Biology*, **276**, 367–373.

Barnosky AD (2008) Megafauna biomass tradeoff as a driver of Quaternary and future extinctions. *PNAS*, **105**, 11543–11548.

Barnosky AD, Koch PL, Feranec RS, Wing SL, Shabel AB (2004) Assessing the causes of late Pleistocene extinctions on the continents. *Science*, **306**, 70–75.

Beaumont MA (2010) Approximate Bayesian computation in evolution and ecology. *Annual Review of Ecology, Evolution and Systematics*, **41**, 379–405.

Brooks N (2006) Cultural responses to aridity in the Middle Holocene and increased social complexity. *Quaternary International*, **151**, 29–49.

de Bruyn M, Hall BL, Chauke LF, Baroni C, Koch PL, Hoelzel AR (2009) Rapid response of a marine mammal species to Holocene climate and habitat change. *PLoS Genetics*, **5**, e1000554.

de Bruyn M, Hoelzel R, Carvalho GR, Hofreiter M (2011) Faunal histories from Holocene ancient DNA. *Trends in Ecology and Evolution*, **26**, 405–413.

Campos P, Willerslev E, Sher A *et al.* (2010) Ancient DNA analyses exclude humans as the driving force behind late Pleistocene musk ox (*Ovibos moschatus*) population dynamics. *PNAS*, **107**, 5675–5680.

Chan YL, Anderson CNK, Hadly EA (2006) Bayesian estimation of the timing and severity of a population bottleneck from ancient DNA. *PLoS Genetics*, **2**, 451–460.

Chikhi L, Sousa VC, Luisi P, Goossens B, Beaumont MA (2010) The confounding effects of population structure, genetic diversity and the sampling scheme on the detection and quantification of population size changes. *Genetics*, **186**, 983–995.

Cohen AS, Stone JR, Beuning KRM *et al.* (2007) Ecological consequences of early Late Pleistocene megadroughts in tropical Africa. *PNAS*, **104**, 16422–16427.

Dadi H, Tibbo M, Takahashi Y, Nomura K, Hanada H, Amano T (2009) Variation in mitochondrial DNA and maternal genetic ancestry of Ethiopian cattle populations. *Animal Genetics*, **40**, 556–559.

Drummond AJ *et al.* (2010) Geneious v5.1. Available from http://www.geneious.com.

Drummond AJ, Rambaut A, Shapiro B, Pybus OG (2005) Bayesian coalescent inference of past population dynamics from molecular sequences. *Molecular Biology and Evolution*, **22**, 1185–1192.

Drummond AJ, Ho SYW, Phillips MJ, Rambaut A (2006) Relaxed phylogenetics and dating with confidence. *PLoS Biology*, **4**, e88.

Dusseldorp GL (2010) Prey choice during the South African Middle Stone Age: avoiding dangerous prey or maximising returns? *African Archaeological Review*, **27**, 107–133.

Endicott P, Ho SYW (2008) A Bayesian evaluation of human mitochondrial substitution rates. *American Journal of Human Genetics*, **82**, 895–902.

Estes RD (1991) *The Behavior Guide to African Mammals*. University of California Press, Berkeley, California, 612 pp.

Excoffier L, Schneider S (1999) Why hunter-gatherer populations do not show signs of Pleistocene demographic expansions. *PNAS*, **96**, 10597–10602.

Excoffier L, Foll M, Petit RJ (2009) Genetic consequences of range expansions. *Annual Review of Ecology, Evolution, and Systematics*, **40**, 481–501.

Faith JT (2008) Eland, buffalo, and wild pigs: were Middle Stone Age humans ineffective hunters? *Journal of Human Evolution*, **55**, 24–36.

Finlay EK, Gaillard C, Vahidi SMF *et al.* (2007) Bayesian inference of population expansions in domestic bovines. *Biology Letters*, **3**, 449–452.

Gignoux CR, Henn BM, Mountain JL (2011) Rapid, global demographic expansions after the origins of agriculture. *PNAS*, **108**, 6044–6049.

Goossens B, Chikhi L, Ancrenaz M, Lackmann-Ancrenaz I, Andau P, Bruford MW (2006) Genetic signature of anthropogenic population collapse in orang-utans. *PLoS Biology*, **4**, 285–291.

Hamilton AC, Taylor D (1991) History of climate and forests in tropical Africa during the last 8 million years. *Climatic Change*, **19**, 65–78.

Heled J, Drummond AJ (2008) Bayesian inference of population size history from multiple loci. *BMC Evolutionary Biology*, **8**, doi:10.1186/1471-2148-8-289.

Heller R, Lorenzen ED, Okello JBA, Masembe C, Siegismund HR (2008) Mid-Holocene decline in Cape buffalo inferred from Bayesian coalescent-based analyses of micro-satellites and mitochondrial DNA. *Molecular Ecology*, **17**, 4845–4858.

Ho SYW, Shapiro B (2011) Skyline-plot methods for estimating demographic history from nucleotide sequences. *Molecular Ecology*, **11**, 423–434.

Ho SYW, Phillips MJ, Cooper A, Drummond AJ (2005) Time dependency of molecular rate estimates and systematic overestimation of recent divergence times. *Molecular Biology and Evolution*, **22**, 1561–1568.

Hoffman JI, Grant SM, Forcada J, Phillips CD (2011) Bayesian inference of a historical bottleneck in a heavily exploited marine mammal. *Molecular Ecology*, **20**, 3989–4008.

Koch PL, Barnosky AD (2006) Late Quaternary extinctions: state of the debate. *Annual Review of Ecology, Evolution and Systematics*, **37**, 215–250.

Li R, Zhu H, Ruan J *et al.* (2010) De novo assembly of human genomes with massively parallel short read sequencing. *Genome Research*, **20**, 265–272.

Lorenzen ED, Nogués-Bravo D, Orlando L *et al.* (2011) Species-specific responses of Late Quaternary megafauna to climate and humans. *Nature*, **479**, 359–365.

MacEachern S, McEwan J, McCulloch A, Mather A, Savin K, Goddard M (2009) Molecular evolution of the Bovini tribe (Bovidae, Bovinae): is there evidence of rapid evolution or reduced selective constraint in Domestic cattle? *BMC Genomics*, **10**, doi:10.1186/1471-2164-10-179.

Martin PS (1984) Prehistoric Overkill: The Global Model. In: *Quaternary Extinctions: A Prehistoric Revolution* (eds Martin PS and Klein RD), pp. 354–403. University of Arizona Press, Tucson, Arizona.

Mayewski PA, Rohling E, Stager JC *et al.* (2004) Holocene climate variability. *Quaternary Research*, **62**, 243–255.

deMenocal PD (2001) Cultural responses to climate change during the late Holocene. *Science*, **292**, 667–673.

deMenocal PD, Ortiz J, Guilderson T, Sarntheim M (2000) Coherent high- and low-latitude climate variability during the Holocene warm period. *Science*, **288**, 2198–2202.

Minin VN, Bloomquist EW, Suchard MA (2008) Smooth skyride through a rough skyline: Bayesian coalescent-based inference of population dynamics. *Molecular Biology and Evolution*, **25**, 1459–1471.

Morin PA, Archer FI, Foote AD, Vilstrup J, Allen EE (2010) Complete mitochondrial genome phylogeographic analysis of killer whales (*Orcinus orca*) indicates multiple species. *Genome Research*, **20**, 908–916.

Nabholz B, Glemin S, Galtier N (2008) Strong variations of mitochondrial mutation rate across mammals—the longevity hypothesis. *Molecular Biology and Evolution*, **25**, 120–130.

Nogués-Bravo D, Ohlemüller R, Batra P, Araújo MB (2010) Climate predictors of Late Quaternary extinctions. *Evolution*, **64**, 2442–2449.

Ogutu JO, Piepho HP, Dublin HT, Bhola N, Reid RS (2008) Rainfall influences on ungulate population abundance in the Mara-Serengeti ecosystem. *Journal of Animal Ecology*, **77**, 814–829.

Okello JBA, Wittemeyer G, Rasmussen HB, Arctander P, Nyakaana S, Douglas-Hamilton I, Siegismund HR (2008) Effective population size dynamics reveal impacts of historic climate events and recent anthropogenic pressure in African elephants. *Molecular Ecology*, **17**, 3788–3799.

Pannell JR (2003) Coalescence in a metapopulation with recurrent local extinction and recolonization. *Evolution*, **57**, 949–961.

Peter MB, Wegmann D, Excoffier L (2010) Distinguishing between population bottleneck and population subdivision by a Bayesian model choice procedure. *Molecular Ecology*, **19**, 4648–4660.

Pond SLK, Posada D, Gravenor MB, Woelk CH, Frost SDW (2006) Automated phylogenetic detection of recombination using a genetic algorithm. *Molecular Biology and Evolution*, **23**, 1891–1901.

Posada D (2008) jModelTest: phylogenetic model averaging. *Molecular Biology and Evolution*, **25**, 1253–1256.

Pritchard JK, Seielstad MT, Perez-Lezaun A, Feldman MW (1999) Population growth of human Y chromosome microsatellites. *Molecular Biology and Evolution*, **16**, 1791–1798.

Rampino MP, Self S (1992) Volcanic winter and accelerated glaciation following the Toba super-eruption. *Nature*, **359**, 50–52.

Ray N, Currat M, Excoffier L (2003) Intra-deme molecular diversity in spatially expanding populations. *Molecular Biology and Evolution*, **29**, 76–86.

Rozas J, Sánches-DelBarrio JC, Messeguer X, Rozas R (2003) DnaSP, DNA polymorphism analyses by the coalescent and other methods. *Bioinformatics*, **19**, 2496–2497.

Rozen S, Skaletsky HJ (2000) Primer3 on the WWW for General Users and for Biologist Programmers. In: *Bioinformatics Methods and Protocols: Methods in Molecular Biology* (eds Krawetz S and Misener S), pp. 365–386. Humana Press, Totowa, New Jersey.

Scheinfeldt LB, Soib S, Tishkoff SA (2010) Working toward a synthesis of archaeological, linguistic, and genetic data for inferring African population history. *PNAS*, **107**, 8931–8938.

Schierup MH, Hein J (2000) Consequences of recombination on traditional phylogenetic analysis. *Genetics*, **156**, 879–891.

Scholz CA, Johnson C, Cohen AS *et al.* (2007) East African megadroughts between 135 and 75 thousand years ago and bearing on early-modern human origins. *PNAS*, **104**, 16416–16421.

Shapiro B, Drummond J, Rambaut A *et al.* (2004) Rise and fall of the Beringian steppe bison. *Science*, **306**, 1561–1565.

Simonsen BT, Siegismund HR, Arctander P (1998) Population structure of Cape buffalo inferred from mtDNA sequences and microsatellite loci: high variation but low differentiation. *Molecular Ecology*, **7**, 225–237.

Sinclair ARE (1977) *The African Buffalo: A Study of Resource Limitation of Populations*. University of Chicago Press, Chicago, Illinois, 355 pp.

Soares P, Alshamali F, Pereira JB *et al.* (2012) The expansion of mtDNA haplogroup L3 within and out of Africa. *Molecular Biology and Evolution*, **29**, 915–927.

Städler T, Haubold B, Merino C, Stephan W, Pfaffelhuber P (2009) The impact of sampling schemes on the site frequency spectrum in nonequilibrium subdivided populations. *Genetics*, **182**, 205–216.

Stanley JD, Krom MD, Cliff RA, Woodward JC (2003) Nile flow failure at the end of the Old Kingdom, Egypt: Strontium isotopic and petrologic evidence. *Geoarchaeology*, **18**, 395–402.

Storz JF, Beaumont MA, Alberts SC (2002) Genetic evidence for long-term population decline in a savannah-dwelling primate: inferences from a hierarchical Bayesian model. *Molecular Biology and Evolution*, **19**, 1981–1990.

Thompson LG, Mosley-Thompson E, Davis ME *et al.* (2002) Kilimanjaro ice core records: evidence of Holocene climate change in tropical Africa. *Science*, **298**, 589–593.

Thompson LG, Mosley-Thompson E, Brecher H *et al.* (2006) Abrupt tropical climate change: past and present. *PNAS*, **103**, 10536–10543.

Tierney JE, Russell JM, Huang Y (2010) A molecular perspective on Late Quaternary climate and vegetation change in the Lake Tanganyika basin, East Africa. *Quaternary Science Reviews*, **29**, 787–800.

Van Hooft WF, Groen AF, Prins HHT (2002) Phylogeography of the Cape buffalo based on mitochondrial and Y-chromosomal loci: Pleistocene origin and population expansion of the Cape buffalo subspecies. *Molecular Ecology*, **11**, 267–279.

Wakeley J (1999) Non-equilibrium migration in human history. *Genetics*, **153**, 1836–1871.

Wakeley J (2001) The coalescent in an island model of population subdivision with variation among demes. *Theoretical Population Biology*, **59**, 133–144.

Wang Z, Shen X, Liu B *et al.* (2010) Phylogeographical analyses of domestic and wild yaks based on mitochondrial DNA: new data and reappraisal. *Journal of Biogeography*, **37**, 2332–2344.

Wegmann D, Leuenberger C, Neuenschwander S, Excoffier L (2010) ABCtoolbox: a versatile toolkit for approximate Bayesian computations. *BMC Bioinformatics*, **11**, 116.

Williams MAJ, Talbot MR (2009) Late Quaternary Environments in the Nile Basin. In: *The Nile: Origin, Environments, Limnology and Human Use* (ed. Dumont HJ), pp. 61–72. Springer Science + Business Media B. V., Dordrecht, Netherlands.

Wolff C, Haug GH, Timmermann A *et al.* (2011) Reduced interannual rainfall variability in East Africa during the Last Ice Age. *Science*, **333**, 743–747.

RH and HRS work on population genetics of large African mammals, with a special emphasis on inferring the demographic history of savannah adapted mammals in response to late Quaternary climate change and human activities. ABO works on population genetics and phylogeography of Australian marsupials, notably the Tasmanian devil.

Data accessibility

DNA sequences: GenBank accessions JQ235505–JQ235547; final partition alignments, sampling localities and BEAST input file (EBSP analysis; concatenated) uploaded as online supplementary material.

Supporting information

Additional supporting information may be found in the online version of this article.

Fig. S1 Scenarios PopulationSizeChanges.

Fig. S2 Skyline plot models compared.

Fig. S3 mtgenome partitions skyline plots.

Fig. S4 EBSPs from random subsamples of the complete data set.

Fig. S5 Livestock population explosion.

Please note: Wiley-Blackwell are not responsible for the content or functionality of any supporting information supplied by the authors. Any queries (other than missing material) should be directed to the corresponding author for the article.